Zhenfeng Wang, Wenyuan Wu*, Xue Bian and Yongfu Wu

Synthesis and characterization of amorphous Al_2O_3 and γ-Al_2O_3 by spray pyrolysis

DOI 10.1515/gps-2015-0128
Received November 13, 2015; accepted February 16, 2016; previously published online May 26, 2016

Abstract: As an environmentally friendly method, spray pyrolysis has been widely used to produce a variety of metal oxides and composite metal oxides. Spray pyrolysis is used to synthesize amorphous Al_2O_3 and γ-Al_2O_3. A pyrolysis temperature ranging from 1073 to 1273 K and a collector temperature ranging from 273 to 283 K result in amorphous Al_2O_3. To strengthen the stability of the amorphous Al_2O_3, La^{3+} was added to modify amorphous Al_2O_3 with different La^{3+} concentrations. With a particle residence time of 2.6–3.0 s in the calciner, the pyrolysis temperature of γ-Al_2O_3 was obtained at 1373 and 1273 K, respectively. Microstructural and morphological analyses conducted by using X-ray diffraction, scanning electron microscopy, high-resolution transmission electron microscopy, and infrared absorption spectrum showed that the obtained alumina are amorphous or γ crystalline forms flake.

Keywords: γ-Al_2O_3; amorphous Al_2O_3; modified lanthanum particles; spray pyrolysis.

1 Introduction

Alumina has abundant applications in the ceramics industry and heterogeneous catalysis, and it has been widely used as absorbents, abrasive materials, ceramics, and biomaterials [1–5]. To achieve such capabilities, alumina should have unique properties, such as high refractive index [6], high dielectric constant, chemical and thermal stability [7], and high transparency [4].

Different and contradictory properties of alumina make it versatile according to our tendency. For example, we can use it for optoelectronic applications; good homogeneity with both good density and dielectric characteristics as well as a low surface roughness [8] make alumina an important material for the ceramic industry. It has been found that amorphous Al_2O_3 has extensive application in catalysis, coatings, microelectronics, and thin film devices because of their chemical, thermal, and mechanical stability [9–11]. At the same time, γ-Al_2O_3 is an important mesoporous material, which has been intensively studied with regard to technical applications as catalysts and catalyst supports [12, 13]. It has been extensively used as advanced catalysts and catalyst supports because of its low cost, good thermal stability, and high specific surface area [14, 15].

Commercial alumina is usually manufactured by the precipitation of aluminum salts [16], sol-gel processing of aluminum alkoxides [17, 18], powder processing technology using various inorganic, and organic aluminum precursors [19–21]. Compared with the previously mentioned method, spray pyrolysis is the result of the decomposition of single inorganic precursors in the air, which is a "green" method. At the same time, hydrogen chloride produced by the exhaust gas is absorbed directly, so the entire process has the advantage of short residence time, high production efficiency, low operating cost, and energy consumption. During the preparation process, atomized droplets of a precursor solution undergo evaporation and shrinkage while flowing through a high-temperature reactor and eventually form particles. Because of evaporation, precipitation, drying, and decomposition occurring in a dispersed phase and a single step, it becomes possible to control the key particle properties (size, morphology, chemical composition, etc.) easily by controlling the process parameters (residence time and decomposition temperature) [22–27]. The spray pyrolysis technique is based on the ultrasonic generation of micrometric-sized aerosol droplets and their decomposition at intermediate temperatures (273–1073 K). Therefore, this method is a continuous flow process and is more economical and more green than other approaches (such as sol-gel processes) that involve multiple steps [28–31].

From an industrial point of view, rare earth elements are important owing to their unique properties and wide range of applications in various fields such as electronics, magnetism, metallurgy, phosphors, catalysts, glass, laser, and ceramic technology [32–34]. Because La^{3+} has

***Corresponding author: Wenyuan Wu,** School of Materials and Metallurgy, Northeastern University, Shenyang 110004, China, e-mail: wuwy@smm.neu.edu.cn
Zhenfeng Wang, Xue Bian and Yongfu Wu: School of Materials and Metallurgy, Northeastern University, Shenyang 110004, China

more structural defects, the addition of La can enhance the thermal stability of γ-Al_2O_3 [35], and it was added in the amorphous Al_2O_3 to study the influence of La on the thermal stability of it.

The present work focuses on the mass production of high surface area Al_2O_3 nanoparticles using inexpensive precursors developed from natural minerals, such as bauxite, and the effect of the precursor on the pore structure of alumina prepared by the spray pyrolysis method [19, 36]. In this work, the amorphous and the gamma crystal types of alumina were obtained by controlling the respective conditions. Microstructural and morphological analyses were conducted by using X-ray diffraction (XRD), scanning electron microscopy (SEM), high-resolution transmission electron microscopy, and infrared (IR) absorption spectrum.

2 Materials and methods

2.1 Amorphous Al_2O_3 particle synthesis

Solutions of $AlCl_3 \cdot 6H_2O$ (AR >99.0%; Sinopharm Chemical Reagent Co. Ltd., Shanghai, China) were used as the precursors. The concentration of the precursors was 20.0 wt%. The schematic representation of the spray pyrolysis equipment (Northeastern University in Shenyang, Liaoning Province, China) shown in Figure 1 is as follows: the spray pyrolysis system consisted of a homemade atomizer, a corundum tube located inside a tubular furnace, three cyclones as the collectors, a gas buffer tank, and a tail gas absorber. Precursor droplets were sprayed by expanding compressed air through the atomizer.

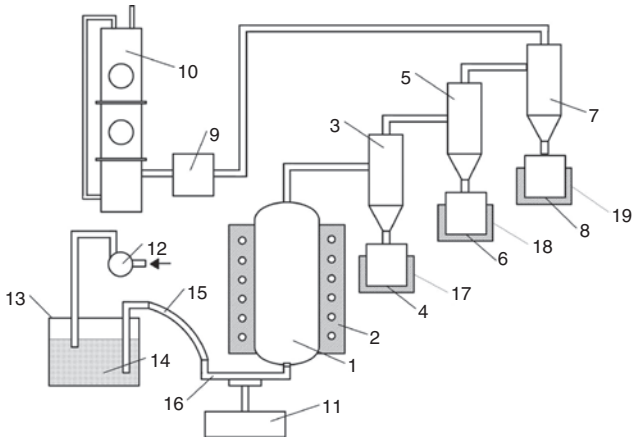

Figure 1: Schematic diagram of automated spray pyrolysis experimental device. (1) Corundum tube, (2) tubular furnace, (3) the first-stage cyclone, (4) the first-stage collector, (5) the second-level cyclone separator, (6) the second-stage collector, (7) the third cyclone, (8) the third-stage collector, (9) flow controllers, (10) tail gas absorber, (11) lifting device, (12) air compressor, (13) into the tank, (14) solution, (15) hose, (16) injection pipe, (17–19) water bath temperature control.

After passing through the diffusion dryer, these partly dried droplets were carried into the corundum tube housed inside the tubular furnace, and the resultant pyrolysate was finally collected by a filter sampler. The temperature of the tubular furnace was controlled and adjusted in the range of 1073–1273 K. Particle residence time in the roaster was controlled by varying the airflow rate from 2.0 to 3.2 l min^{-1}, corresponding to a residence time of 0.7–1.0 s and a collector temperature of 273–278 K by an ice water bath.

2.2 La^{3+}-modified amorphous Al_2O_3 particles

Solutions of $AlCl_3 \cdot 6H_2O$ and $LaCl_3 \cdot 6H_2O$ (AR, >99.0%; Sinopharm Chemical Reagent Co. Ltd.) were used as the precursors. The concentration of the $AlCl_3$ was 20.00 wt% and $LaCl_3$ was 0.23 wt%, 0.46 wt%, 0.63 wt%, the detailed synthesis process was given in the preceding paragraph, and the roasting temperature was controlled and adjusted in 1073 K, with a residence time of 0.7–1.0 s and a collector temperature of 293–318 K.

2.3 γ-Al_2O_3 particle synthesis

The detailed synthesis process was given in the Figure 1, and the roasting temperature was controlled and adjusted in the range of 1173–1373 K, with a residence time of 2.6–3.0 s and a collector temperature of 293–318 K.

2.4 Characterization of prepared particles

The crystalline structure of the products was determined by a powder XRD (X'Pert Pro, PANalytical Corporation, The Netherlands) with Cu Kα [33, 34] radiation (λ=0.154 nm) at 40 kV and 40 mA. The scan rate was 4° 2θ·min^{-1}, and the scan ranged from 10° to 90° 2θ. Peak positions and relative intensities were characterized by comparison with the International Centre for Diffraction Data files. IR spectra were measured with a Perkin Elmer Spectrum GX Fourier transform-infrared spectrometer (IRAffinity-1, Shimadzu, Japan). The transmission electron microscope (TEM) examinations were performed using a TEM instrument (Tecnai G220; FEI, Hillsboro, OR, USA) operating at 200 kV. Al_2O_3 samples were collected directly onto Cu microgrids, and a droplet of suspending liquid was deposited onto a Cu microgrid and allowed to dry. SEM images were obtained on a Zeiss ULTRA plus SEM (Zeiss Ultra Plus, Zeiss, Oberkochen, Germany) equipped with energy-dispersive X-ray spectroscopy (EDS), which was used to observe the SEM microstructure.

3 Results and discussion

Figure 2 shows the XRD patterns of samples obtained by pyrolysis at different temperatures. It can be seen that the XRD patterns consist of three broad diffuse peaks between diffraction angles 20° and 80°. The sample obtained at a temperature of 1073 K (Figure 2A) shows some small shape peak, which indicates some crystalline phase mixed with the primary amorphous structures. When the pyrolysis

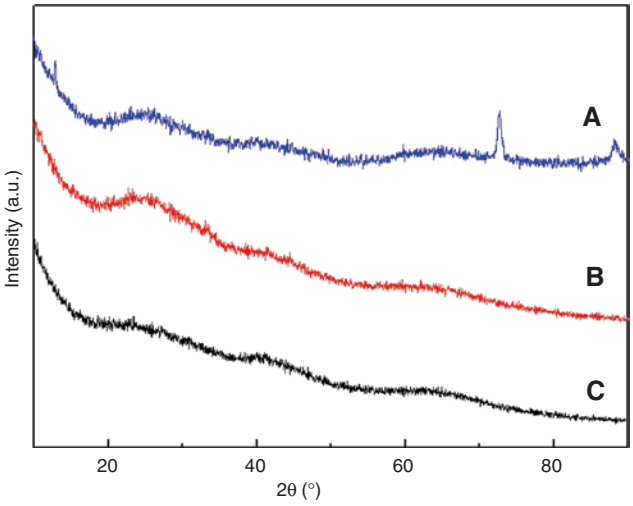

Figure 2: XRD patterns of amorphous Al_2O_3 at different pyrolysis temperatures: (A) 1073 K, (B) 1173 K, (C) 1273 K, collector temperature at 273–283 K, and particle residence time in the calciner for 0.7–1.0 s.

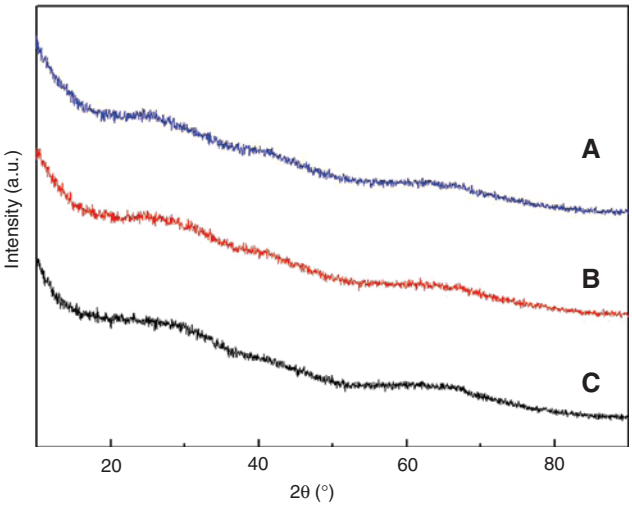

Figure 3: XRD patterns of amorphous Al_2O_3 modified by different La^{3+} concentrations (A) LaOCl 1 wt%, (B) LaOCl 2 wt%, (C) LaOCl 3 wt%, pyrolysis temperatures of 1073 K, collector temperature of 273–283 K, particle residence time of 0.7–1.0 s.

temperature is up to 1173 and 1273 K, there is no apparent crystalline phase corresponding to the sharp crystallization peak in (Figure 2B and C), indicating that this sample is in the amorphous structures. As the pyrolysis temperature is 1173 K, its pattern shows broad diffuse backgrounds, but the amorphous diffuse peak is shape, and the amorphous diffuse peak of 1173 K is sharper than that of 1273 K, showing that it has the trend of further crystallization. Thus, the threshold overheating temperature for the fully amorphous structure of amorphous Al_2O_3 is at least 1173 K, below which it may have an intersection with the crystallization position.

Figure 3 depicts XRD patterns of the Al_2O_3 particles modified by La^{3+}, and no crystalline peak is detected from all particles obtained with each La^{3+} concentration. Thus, the particles can be considered as amorphous structure because La^{3+} has more structural defects, which can effectively improve the stability of amorphous Al_2O_3.

Figure 4 presents the XRD patterns of γ-Al_2O_3 at different pyrolysis temperatures. As the pyrolysis temperatures are 1373 and 1273 K, their pattern peaks are identified as γ-Al_2O_3 peaks at 19.44°, 37.59°, 39.47°, 45.84°, and 67.00°. When the pyrolysis temperature is down to 1173 K, there is no apparent crystalline phase corresponding to the sharp γ-Al_2O_3 peak, indicating that this sample have a certain percentages of the amorphous structure.

Figure 5 shows that the TEM images of the amorphous Al_2O_3 (Figure 5A and B) were obtained at a pyrolysis temperature of 1273 K, a residence time of 0.7–1.0 s, a collector temperature of 273–278 K by ice water bath and

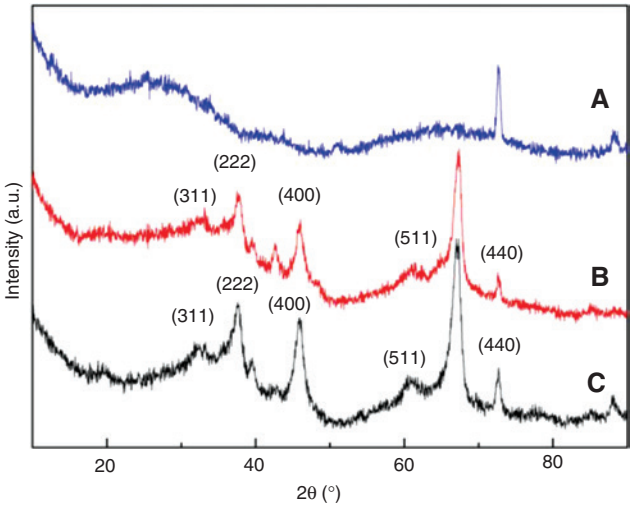

Figure 4: XRD patterns of γ-Al_2O_3 at different pyrolysis temperatures: (A) 1173 K, (B) 1273 K, (C) 1373 K, collector temperature of 293–318 K, and particle residence time of 0.7–1.0 s.

γ-Al_2O_3 (Figure 5C and D) at pyrolysis temperature 1373 K, a residence time of 2.6–3.0 s, and a collector temperature of 293–318 K by water bath. It can be seen from the TEM images that the Al_2O_3 particles exhibit a flake particle with a particle size distribution between 5 and 20 μm. The main reason is that droplets would turn into spherical shells at a high temperature, and these shells may burst into fragments because of the gas generated in them. In Figure 5B, the diffraction pattern is an amorphous ring proving that alumina crystals did not grow, which is consistent with

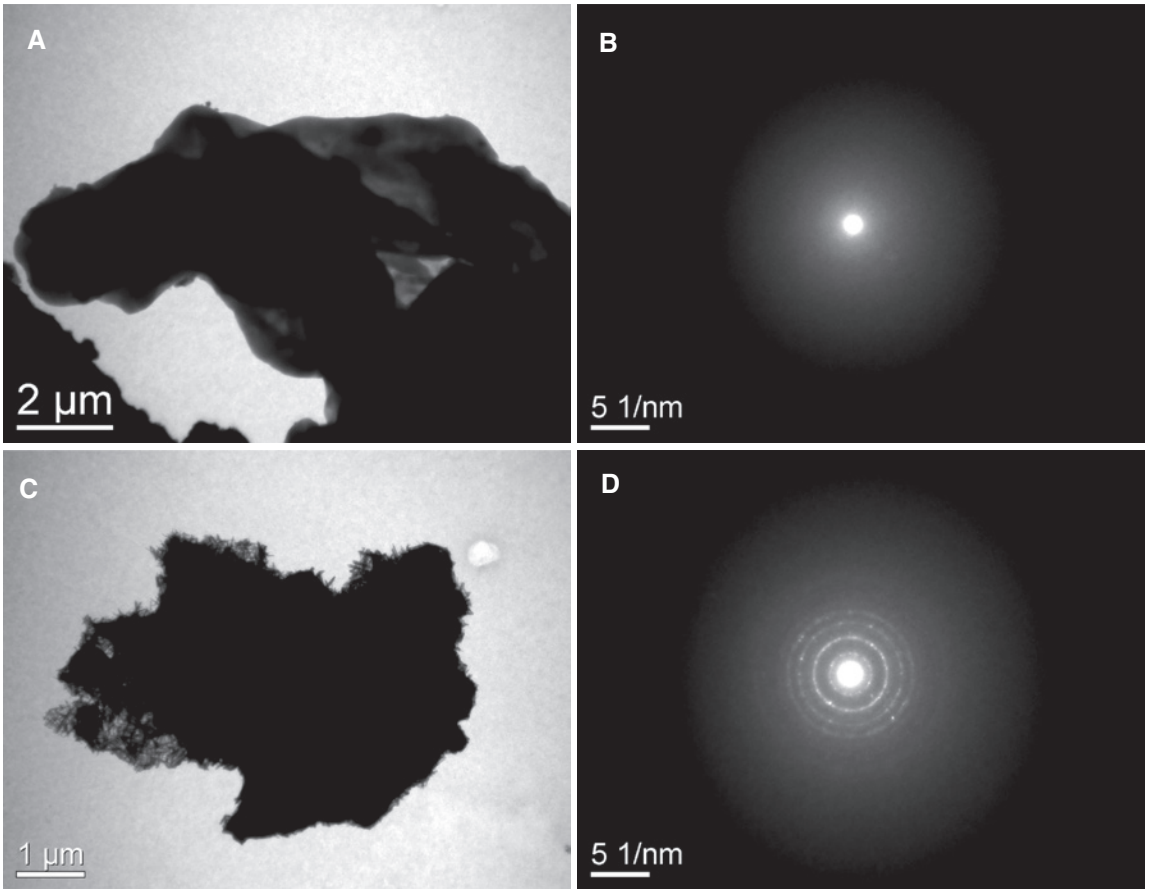

Figure 5: TEM images and SAED patterns of the amorphous Al_2O_3 at 1273 K (A and B) and γ-Al_2O_3 samples at 1373 K (C and D).

XRD diffraction diagram. Figure 5D shows a selected area electron diffraction pattern taken from the sample with a pyrolysis temperature of 1373 K and a residence time of 2.6–3.0 s, indexed in accordance with the γ-Al_2O_3 phase (JCPDS=29-0063), having a defect spinel structure [37, 38].

The FT-IR spectra of amorphous Al_2O_3 prepared by spray pyrolysis are shown in Figure 6. The band at 3457 cm^{-1} is due to the stretching mode of hydroxyl groups (from surface water and adsorbed water). The band at 1643 cm^{-1} is due to the bending mode of water molecules, and the content forms La^{3+} during the Al_2O_3. Then the hydrolysis of the La^{3+} cation takes place, and the resulting protons generate Brønsted acid sites. Therefore, the amount of Brønsted acid sites is increased. The broad band at 755 cm^{-1} can be ascribed to the Al-O vibration of (AlO_4) [39, 40]. As La is added in the aluminum chloride solution, pyrolysis occurs at 1073 K instead of crystallization. Therefore, adding La can effectively inhibit crystallization because of slow cooling. The experimental results are consistent with XRD analysis.

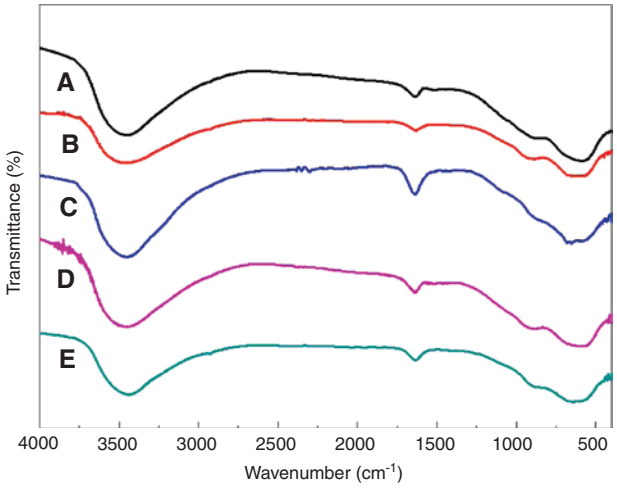

Figure 6: FT-IR spectra of amorphous Al_2O_3 (A) pyrolysis temperature at 1273 K, residence time of 0.7–1.0 s, collector temperature of 273–278 K; (B) 1173, 0.7–1.0 s, 273–283 K; (C) 1073, 0.7–1.0 s, 273–283 K, LaOCl 3 wt%; (D) 1073, 0.7–1.0 s, 273–283 K, LaOCl 2 wt%; (E) 1073, 0.7–1.0 s, 273–283 K, LaOCl 1 wt%.

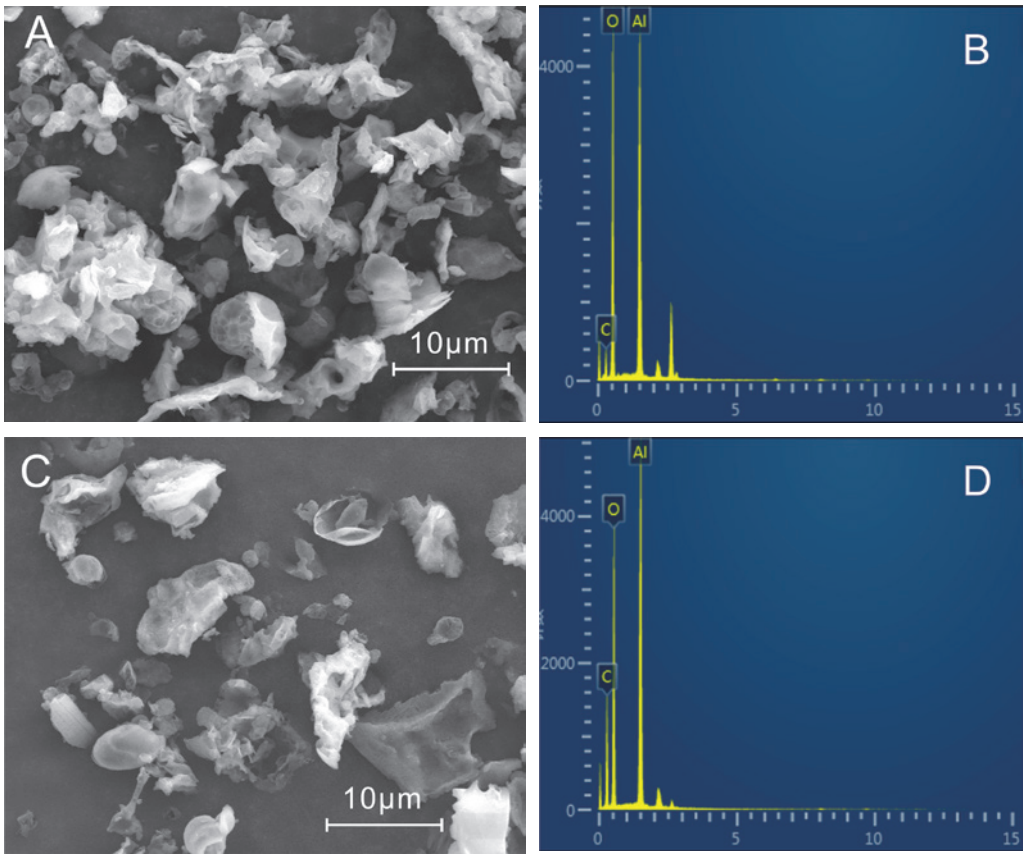

Figure 7: SEM images and EDS patterns of the amorphous Al_2O_3 at 1273 K (A and B) and γ-Al_2O_3 samples at 1373 K (C and D).

The SEM images and the EDS patterns of the amorphous Al_2O_3 and γ-Al_2O_3 are shown in Figure 7. We can see that the Al_2O_3 sample is a flake particle with a particle size distribution between 5 and 20 μm, which is consistent with the TEM images. The EDS examination confirms the presence of Al and O from the sample, and the existence of C elements is due to the conductive adhesive.

4 Conclusions

By changing the pyrolysis temperature, the particle residence time in the roaster, and the temperature of the collector, the amorphous Al_2O_3 and the γ crystal structure of Al_2O_3 were successfully prepared by spray pyrolysis. The effect of the pyrolysis temperature, the particle residence time in the roaster, and the temperature of the collector on the crystal shape is very obvious. Previous studies showed that La^{3+} can effectively improve the stability of the γ-Al_2O_3, and it was found to be helpful to the stability of the amorphous Al_2O_3 in this work. The proposed spray pyrolysis to synthetic Al_2O_3 was simple, cheap, efficient, and free of pollution, which makes it very suitable for scale-up production. Furthermore, $LaAlO_3$ can be made with amorphous Al_2O_3 and microcrystalline LaOCl solid solution precursor by this "green" synthetic method, which will be mentioned in another article.

Acknowledgments: This work was financially supported by the National Natural Science Foundation of China (grant no. 51274060).

References

[1] Costina I, Franchy R. *Appl. Phys. Lett.* 2001, 78, 4139–4141.
[2] Ealet B, Elyakhloufi MH, Gillet E, Ricci M. *Thin Solid Films*. 1994, 250, 92–100.
[3] Shamala KS, Murthy LCS, Narasimha Rao K. *Mater. Sci*. 2004, 27, 295–301.
[4] He H, Zhang X, Wu Q, Zhang C, Yu Y. *Catal. Surv. Asia*. 2008, 12, 38–55.
[5] Nassar NN, Hassan A, Pereira-Almao P. *J. Colloid. Interf. Sci*. 2011. 360, 233–238.
[6] Yamaguchi N, Tadanaga K, Matsuda A, Minami T, Tatsumisago M. *Thin Solid Films*. 2007, 515, 3914–3917.

[7] Klein TM, Niu D, Epling WS, Li W, Maher DM, Hobbs CC, Hegde RI, Baumvol IJR, Parsons G. *Appl. Phys. Lett*. 1999, 75, 4001–4003.
[8] Aguilar-Frutis M, Garcia M, Falcony C, Plesch G, Jimenez-Sandoval S. *Thin Solid Films*. 2001, 389, 200–206.
[9] Chang H, Choi Y, Kong K, Ryu B-H. *Chem. Phys. Lett*. 2004, 391, 293–296.
[10] Lin C, Yu M, Cheng Z, Zhang C, Meng Q, Lin J. *Inorg. Chem*. 2008, 47, 49–55.
[11] Freund HJ, Pacchioni G. *Chem. Soc. Rev*. 2008, 37, 2224–2242.
[12] Bagshaw SA, Prouzet E, Pinnavaia TJ. *Science*. 1995, 269, 1242–1244.
[13] Zhao D, Huo Q, Feng J, Chmelka BF, Stucky GD. *J. Am. Chem. Soc*. 1998, 120, 6024–6036.
[14] Kasprzyk-Hordern B. *Adv. Colloid Interface Sci*. 2004, 110, 19–48.
[15] Trueba M, Trasatti SP. *Berichte Der Deutschen Chemischen Gesellschaft*. 2005, 2005, 3393–3403.
[16] Delmon, B. *Formation of Final Catalyst*, Wiley-VCH Verlag GmbH: Weinheim, Germany, 2008, 541–579.
[17] Komarneni S. *J. Sol-Gel Sci. Technol*. 1996, 6, 127–138.
[18] Xiao FS, Qiu S, Pang W, Xu R, *ChemInform*. 1999, 30, 1091–1099.
[19] Manivasakan P, Karthik A, Rajendran V. *Powder Technol*. 2013, 234, 84–90.
[20] Pratsinis SE. *Prog. Energy Combust. Sci*. 1998, 24, 197–219.
[21] Tani T, Takatori K, Pratsinis SE. *J. Am. Ceram. Soc*. 2004, 87, 523–525.
[22] Castañeda L, Alonso JC, Ortiz A, Andrade E, Saniger JM, Bañuelos JG. *Mater. Chem. Phys*. 2003, 77, 938–944.
[23] Fukui T, Ohara S, Naito M, Nogi K. *J. Eur. Ceram. Soc*. 2003, 23, 2963–2967.
[24] Ibáñez RL, Barrado JRR, Martín F, Brucker F, Leinen D. *Surf. Coat. Tech*. 2004, 188–189, 675–683.
[25] Koch W, Friedlander SK. *Part. Part. Syst. Char*. 1991, 8, 86–89.
[26] Martín MI, Rabanal ME, Gómez LS, Torralba JM, Milosevic O. *J. Eur. Ceram. Soc*. 2008, 28, 2487–2494.
[27] Vallet-Regí M, Rodríguez-Lorenzo LM, Ragel CV, Salinas AJ, González-Calbet JM. *Solid State Ionics*. 1997, 101–103, Part 1, 197–203.
[28] Mueller R, Mädler L, Pratsinis SE, *Chem. Eng. Sci*. 2003, 58, 1969–1976.
[29] Okuyama K, Lenggoro IW, *Chem. Eng. Sci*. 2003, 58, 537–547.
[30] Widiyastuti W, Balgis R, Iskandar F, Okuyama K, *Chem. Eng. Sci*. 2010, 65, 1846–1854.
[31] Rosner DE. *Ind. Eng. Chem. Res*. 2005, 44, 6045–6055.
[32] Jia Q, Li H, Tong S, Li Z, Zhou W, Meng S. *Sep. Purif. Technol*. 2009, 64, 345–350.
[33] Yin S, Wu W, Bian X, Luo Y, Zhang F. *Ind. Eng. Chem. Res*. 2013, 52, 8558–8564.
[34] Yin SH, Li SW, Wu WY, Bian X, Peng JH, Zhang LB. *RSC Adv*. 2014, 4, 59997–60001.
[35] Lafarga D, Lafuente A, Menéndez M, Santamara J. *J. Membrane Sci*. 1998, 147, 173–185.
[36] Liu C, Liu Y, Ma Q, Ma J, He H. *Ind. Eng. Chem. Res*. 2013, 53, 13377–13383.
[37] Paglia G, Rohl AL, Buckley CE, Gale JD. *Phys. Rev. B*. 2005, 71, 224115.
[38] Zhou RS, Snyder RL. *Acta Crystallogr.* 1991, 47, 617–630.
[39] Lange NA, Speight JG. *Lange's Handbook of Chemistry*. 16th ed. McGraw-Hill, New York, 2005.
[40] Lin C, Zhang C, Lin J. *J. Phys. Chem. C*. 2007, 111, 18148–18154.

Bionotes

Zhenfeng Wang

Zhenfeng Wang is a PhD student at the Northeastern University in China. His primary research interests include rare earth chloride and aluminum chloride spray pyrolysis and the preparation of rare earth oxide materials.

Wenyuan Wu

Wenyuan Wu is a professor and a PhD supervisor at the Northeastern University. His research interests include hydrometallurgy and precious metals metallurgy technology and application.

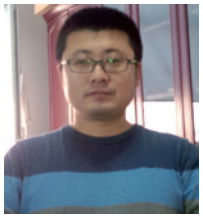

Xue Bian

Xue Bian is an associate professor and a master's supervisor at the Northeastern University. His research interests include rare metal metallurgical technology and application, comprehensive use of green technology, and rare earth resources.

Yongfu Wu

Yongfu Wu is a PhD student at the Northeastern University in China and an associate professor and a master's supervisor at the Inner Mongolia University of Science and Technology. His research interests include rare earth metallurgy process simulation and optimization.